ADVANCED FUNCTIONAL MATERIALS
www.afm-journal.de

Dynamic Microcapsules with Rapid and Reversible Permeability Switching

*Jörg G. Werner, Brendan T. Deveney, Saraf Nawar, and David A. Weitz**

Dynamic microcapsules are reported that exhibit shell membranes with fast and reversible changes in permeability in response to external stimuli. A hydrophobic anhydride monomer is employed in the thiol–ene polymerization as a disguised precursor for the acid-containing shells; this enables the direct encapsulation of aqueous cargo in the liquid core using microfluidic fabrication of water-in-oil-in-water double emulsion drops. The poly(anhydride) shells hydrolyze in their aqueous environment without further chemical treatment, yielding cross-linked poly(acid) microcapsules that exhibit trigger-responsive and reversible property changes. The microcapsule shell can actively be switched numerous times between impermeable and permeable due to the exceptional mechanical properties of the thiol–ene network that prevent rupture or failure of the membrane, allowing it to withstand the mechanical stresses imposed on the capsule during the dynamic property changes. The permeability and molecular weight cutoff of the microcapsules can dynamically be controlled with triggers such as pH and ionic environment. The reversibly triggered changes in permeability of the shell exhibit a response time of seconds, enabling actively adjustable release profiles, as well as on-demand capture, trapping, and release of cargo molecules with molecular selectivity and fast on-off rates.

1. Introduction

Encapsulation in microcapsules for the protection and delivery of active substances is widely employed in agriculture, cosmetics, drug delivery, detergents, and food additives, benefiting from the separation of the liquid cargo and solid encapsulant as well as high cargo content.[1–5] Stimuli-responsive shell materials provide control over when cargo is released with triggers such as pH, shear, light, and temperature.[6–8] Most microcapsules are unidirectional and single-use delivery vehicles, because of their irreversible and destructive release mechanisms through shell degradation or rupture; once release is initiated, it cannot be stopped or reversed.[9,10] In many advanced applications, however, microcapsules would benefit from the ability to transiently release their cargo in response to changes in their environment but remain shut off otherwise, and to repeatedly cycle between these two states. For example, injectable therapeutic reservoirs that release drugs on-demand, such as insulin only under high glucose levels or anti-inflammatories when inflammation symptoms occur in the surrounding tissue, significantly decrease the number of drug injections needed for treatment.[11–14] One way to achieve such injectable on-demand release systems is the use of dynamically responsive permeability, which is unattainable in common microcapsules due to their inability to reversibly and quickly adjust their shell's permeability to changes in stimuli. The ability to switch between permeable and impermeable states further enables the capture of molecular species from the surrounding medium and trap them inside the capsule core. For example, water treatment and purification could benefit from such passive microtraps for the removal of harmful molecular species. Commonly employed flat membranes require flux of the water through the membrane to remove molecular impurities, which is slow due to the small pore sizes needed.[15] Microencapsulants that trap molecular impurities are easier to remove, since they are orders of magnitude larger than the target molecules.[16] Microcapsules with dynamically tunable permeability dispersed in waste water could capture molecular species in their core when the shell is permeable, trap them by switching permeability off, and subsequently be removed together with the trapped molecular impurities by simple microfiltration. The development of microcapsules that rapidly and distinctly change their permeability requires shell materials that alter their physicochemical properties fast and without rupture under the inevitable resultant mechanical stresses; most microcapsules break when triggered to release or upon reversal of the trigger because of insufficient mechanical and chemical stability and, therefore, cannot be reloaded or used as an on-demand releasing reservoir.[17] To date, however, microcapsules with reversibly trigger-responsive shell membranes directly fabricated around water drops have not been obtained.[13,18–24] Such dynamic responsiveness in microcapsules is highly desirable though,

Dr. J. G. Werner, B. T. Deveney, S. Nawar
John A. Paulson School of Engineering
Harvard University
Cambridge, MA 02138, USA
Prof. D. A. Weitz
John A. Paulson School of Engineering and Applied Sciences
and Department of Physics
Harvard University
Cambridge, MA 02138, USA
E-mail: weitz@seas.harvard.edu
The ORCID identification number(s) for the author(s) of this article can be found under https://doi.org/10.1002/adfm.201803385.

DOI: 10.1002/adfm.201803385

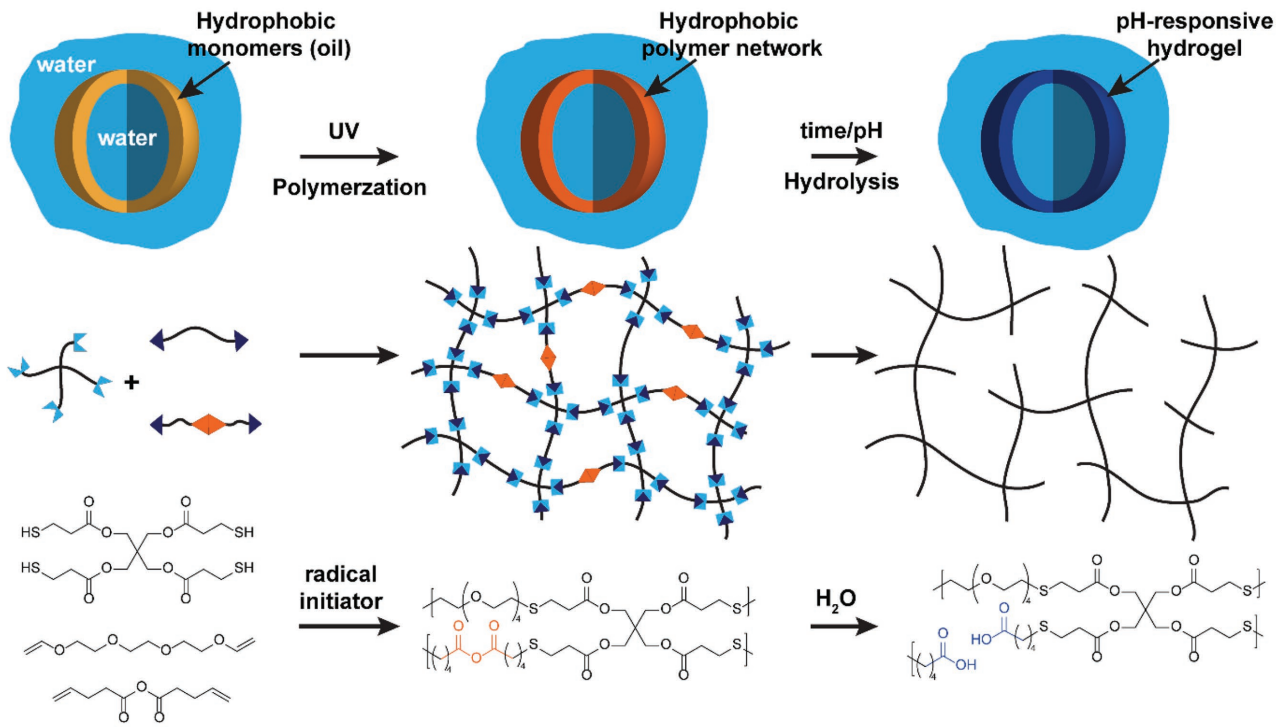

Scheme 1. Illustration and molecular structure of double emulsion drops with thiol–ene monomer shells, and their conversion to poly(anhydride) and reversibly responsive poly(acid) microcapsules.

as it enables qualitatively new ways for their utilization and employment.

Here, we report the fabrication of robust microcapsules that exhibit a reversible, triggerable, nondestructive, and rapid transition between permeable and impermeable states. We employ the microfluidic fabrication of double emulsion drops for the direct encapsulation of aqueous drops in anhydride-containing monomer shells.[25,26] The anhydride serves as the hydrophobic acid precursor for the direct emulsion synthesis of a shell containing functional acid moieties around a water core. The double emulsion drops are converted to poly(anhydride) microcapsules with a water core through thiol–ene polymerization. The poly(anhydride) shell hydrolyzes in its aqueous environment without additional chemical treatment,[14,27,28] yielding cross-linked poly(acid) microcapsules, as illustrated in **Scheme 1**. The weak acidity of the thiol–ene shells with tethered carboxylic acids renders the microcapsules responsive to pH and ionic environment; they turn highly hydrophilic and permeable when swollen through deprotonation at high pH, and hydrophobic and impermeable when deswollen upon protonation or ionic cross-linking. The trigger-responsive change in hydrophilicity of the shells is rapid, switching between permeable to impermeable within seconds. The trigger-responsive change in hydrophilicity of the shells is also reversible, maintaining the microcapsules' structural integrity for repeated cycling between the two states. The molecular weight cutoff (MWCO) and release rate are tunable over a wide range through tuning shell composition and mesh size, while the dynamically triggerable change in permeability enables the active adjustment of release in time with fast response rates; the diffusion in and out of the core can be repeatedly enabled and disabled with changing stimuli. Additionally, the mechanically and chemically robust polymeric thiol–ene network provides sufficient stability for repeated permeability change, enabling the microcapsules to be reloaded and reused numerous times, as demonstrated by repeated capture-trap-release cycles.

2. Results and Discussion

2.1. Fabrication and Characterization of Poly(anhydride) Microcapsules

To form the stimuli-responsive polymeric networks in the microcapsule shell, we employ multifunctional thiols and olefins as monomers in a thiol–ene step-growth polymerization. Pentaerythritol tetra(mercaptopropionate) (PETMP) as a tetrafunctional thiol is polymerized with the difunctional comonomers triethyleneglycol divinylether (TEGDVE) as a permanent cross-linker and pentenoic anhydride (PenAn) as a transient cross-linker and acid source, as depicted in Scheme 1. The thiol–ene monomers are water immiscible liquids and used as the oil phase in water-in-oil-in-water (W/O/W) double emulsion drops to fabricate microcapsules with cross-linked poly(anhydride) shells. Capsules with low, medium, and high anhydride content are fabricated with comonomer ratios of 6:1, 2:1, and 4:6, respectively, between the permanent cross-linking agent TEGDVE and the hydrolyzable PenAn, to study the influence of composition on the microcapsule properties.

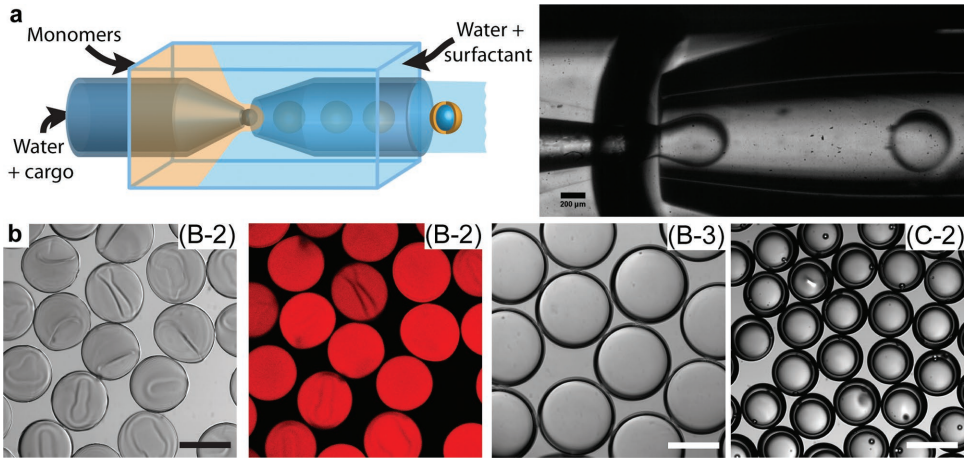

Figure 1. a) Schematic illustration and optical microscopy image of the double emulsion drop fabrication in a glass capillary microfluidic device. b) Optical (first, third, fourth) and fluorescence confocal microscopy images (second) of poly(anhydride) microcapsules with various sizes and shell thickness. B-2 contains sulforhodamine B in its aqueous core. Note that the buckling of the thin-shelled capsules (B-2) is due to osmotic imbalance between the inner and outer aqueous phase prior to fabrication. Labels correspond to entries in Table 1. Scale bars are 200 µm.

Higher anhydride content yields microcapsules with lower cross-link density and higher acid content upon hydrolysis.

Homogenous W/O/W double emulsion drops are fabricated in glass capillary microfluidic devices.[29,30] Microfluidic drop making enables the production of microcapsules with complete encapsulation and precise control over diameter and shell thickness.[29,31] The devices consist of two cylindrical capillaries with hydrophobic and hydrophilic surface treatment for inlet and outlet, respectively, which are inserted into opposite ends of a square capillary, as illustrated and shown in **Figure 1**a. Double emulsion drops are formed between the tapered tips of the inlet and outlet capillaries and the monomer shell is polymerized by exposure of the double emulsion drops to UV light immediately after formation. The resultant water-dispersed microcapsules with a hydrophobic polymer shell surrounding an aqueous core exhibit homogenous size with low polydispersity and tunable shell thickness that is controlled by the flow rates and device design, as shown in Figure 1b, Figure S1 (Supporting Information), and summarized in **Table 1**. The thin-shelled capsules show buckled morphologies due to an osmotic imbalance between the inner and outer aqueous phase prior to fabrication, causing water to diffuse from the core of the microcapsules to the continuous phase to mitigate the osmotic pressure. The reduction in core volume due to the water egress causes the shells of the capsules to buckle. The fabrication of double emulsion drops in microfluidic glass capillary devices with various shell thicknesses is shown in Videos S1–S3 (Supporting Information).

2.2. Conversion of Poly(anhydride) to Poly(acid) Microcapsules

The transient anhydride cross-linker hydrolyzes with water to form two carboxylic acid groups tethered to the polymeric shell network. Hence, the hydrolysis of the anhydride causes an increase in mesh size of the polymeric network, as illustrated in Scheme 1. The increase in mesh size is accompanied by a change in hydrophilicity of the polymer network due to the formation of polar carboxylic acid functional groups. Before hydrolysis, the poly(anhydride) shells are impermeable to small hydrophilic molecules such as the fluorophore sulforhodamine B, as shown in Figure 1b and Figure S1d–j (Supporting Information). Upon hydrolysis, the resulting poly(acid) network exhibits an increased mesh size and hydrophilicity, causing the shell to swell with water and allowing sulforhodamine B to diffuse through the shell membrane, enabling its use as a fluorescent probe to indicate the completion of the shell's hydrolysis.

Table 1. Composition, fabrication parameters, and sizes of poly(anhydride) microcapsules.

Entry No.	Cross-link density	Mol% pentenoic anhydride in monomer mixture	Mol% pentanoic acid in hydrolyzed gel	Shell-type	Flow rates (O-M-I) [mL h^{-1}]	Diameter[a)] [µm]
A-1	High	14.3%	25.0%	Thin	12-0.4-1	382 ± 11
B-1	Medium	33.3%	50.0%	Thin	12-0.5-0.5	374 ± 10
B-2	Medium	33.3%	50.0%	Thin	15-0.8-0.6	221 ± 6
B-3	Medium	33.3%	50.0%	Thick	15-0.4-1.6	316 ± 7
C-1	Low	60.0%	75.0%	Thin	12-0.4-1	383 ± 7
C-2	Low	60.0%	75.0%	Thick	20-2-1	178 ± 2

[a)]Geometrical average ± standard deviation of the diameter of over 25 capsules for thick-shelled capsules and of 2D projection from at least three thin-shelled, buckled capsules.

The time it takes to fully hydrolyze the shell is tunable through its chemical composition, thickness, and the pH of the surrounding aqueous medium, enabling precise control over release time from the poly(anhydride) microcapsules. To demonstrate the control over hydrolysis rate through composition, we fabricated microcapsules of similar size but with different anhydride content. They are loaded with sulforhodamine B and exposed to phosphate buffered saline (PBS) with a pH of 7.4. Capsules with high anhydride content are hydrolyzed completely to poly(acid) microcapsules within 2 d as indicated by the release of sulforhodamine B. After the same time, only some of the microcapsules with medium anhydride content are hydrolyzed, while none of the microcapsules with low anhydride content have released their fluorescent cargo. For these microcapsules up to 4 and 6 d, respectively, are required to fully hydrolyze the shells to poly(acid) networks and release the encapsulated sulforhodamine B, as shown in **Figure 2**a and Figure S2 (Supporting Information). The trend of faster hydrolysis rate with higher anhydride content is due to the networks surface-initiated hydrolysis.[27] The amount of water at the advancing hydrolysis front and hence the hydrolysis rate is higher for materials with higher acid content after conversion. Additionally, the microcapsules with the highest anhydride content increase in size during hydrolysis in PBS buffer at a pH of 7.4, in contrast to the capsules with low and medium anhydride content. We assume that the pKa of the poly(acid) network decreases with increasing acid content, causing some of the carboxylic acid units in the microcapsules with high acid content to be deprotonated and the polymer shells to swell.

The hydrolysis of the poly(anhydride) microcapsules is further confirmed using IR spectroscopy. The conversion of the anhydrides to carboxylic acids introduces hydroxyl groups that yield a broad absorption band in the IR spectrum at wavenumbers above 3100 cm^{-1}. Microcapsules with higher anhydride content exhibit larger absorption in this OH-stretching region of the IR spectrum after hydrolysis, as shown in Figure 2b. Shell thickness of the poly(acid) microcapsules is tunable between a few micrometers to tens of micrometers depending on drop fabrication design and flow rates, as shown in the scanning electron microscopy (SEM) images in Figure 2c–e. The aqueous core is not centered in the double emulsion drop due to the density mismatch with the monomer shell, leading to asymmetric microcapsules with nonuniform shell thickness that is particularly apparent for thick-shelled capsules (Figure 2d,e). For example, microcapsules with a core-to-shell volume ratio of 4 exhibit a shell thickness of 5 and 15 µm on the thin and thick side of the capsule, respectively.

The onset of cargo release from the poly(anhydride) microcapsules is also controllable by the pH of the surrounding aqueous medium, since hydrolysis is accelerated catalytically in acidic and basic conditions. Microcapsules with medium anhydride content hydrolyze within hours at pH 11, but take days at

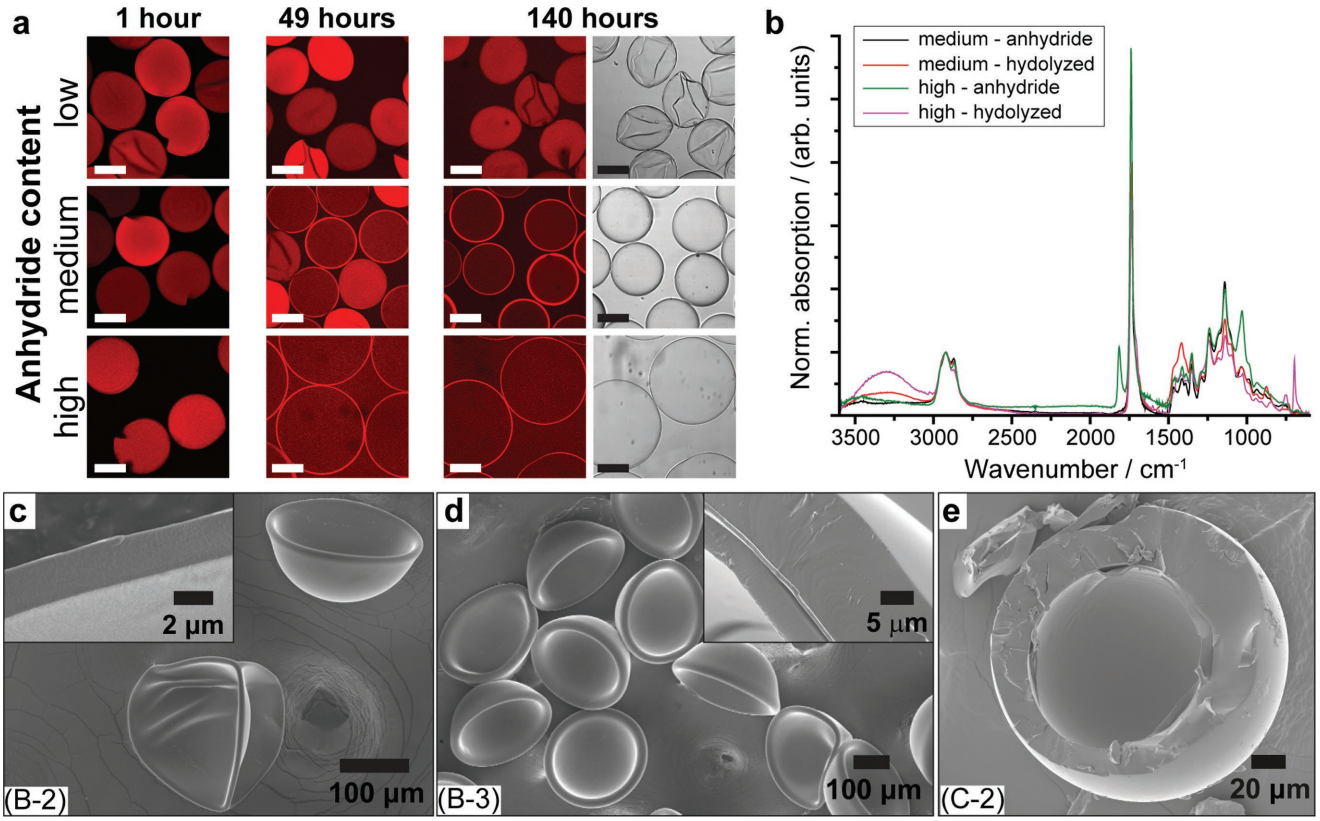

Figure 2. a) Fluorescence confocal (column 1–3) and optical (column 4) microscopy images of poly(anhydride) microcapsules during hydrolysis in PBS buffer at pH = 7.4 for different anhydride content (entries A-1, B-1, C-1 in Table 1). Scale bars are 200 µm. b) ATR-FT-IR spectra of poly(anhydride) microcapsules before (anhydride) and after hydrolysis in PBS buffer. c–e) Scanning electron microscopy images of thin-shelled and thick-shelled poly(acid) microcapsules. Insets show cross sections of the shells. Labels correspond to entries in Table 1.

pH 2, and exhibit the slowest hydrolysis rate and release time in noncatalytic deionized (DI) water, as shown in Figure S3 (Supporting Information). The hydrolysis and release time is further controlled with the shell thickness; thicker shells take longer to fully hydrolyze and become permeable, as shown in Figure S4 (Supporting Information). Hence, the onset time for the release of aqueous cargo from the poly(anhydride) microcapsules is independently tunable from hours to days through chemical composition, shell thickness, and pH.

2.3. pH-Responsive Properties of the Dynamic Microcapsules

The hydrolyzed microcapsules are reversibly stimuli-responsive, enabling dynamic control over their size and permeability. The shells contain tethered carboxylic acids that render them responsive to external triggers such as pH and ionic environment. At neutral and low pH, the polyacids are protonated and the microcapsule shells are hydrophobic. With increase of the pH in the surrounding aqueous medium, the acid groups are deprotonated yielding charged polyelectrolyte networks that swell significantly with water; the result is an increase in shell volume and microcapsule size. The increase in capsule size is not predominantly driven by an increase in shell thickness but is caused by the in-plane expansion of the poly(acid) shell that significantly increases the capsule surface area. Thus, the microcapsule size increases to accommodate the difference in its surface area imposed by the swelling of the shell. In contrast, common pH-responsive microgels swell homogenously in the entire volume of the microparticle. The poly(acid) microcapsules exhibit a significant difference in size between pH 9 and 7, indicating the threshold pH for the hydrophilicity switch. The difference in size is controlled by the cross-link density, with larger swelling for lower cross-link density, as summarized in **Figure 3**a. Microcapsules with low cross-link density demonstrate a factor of 2.3 difference in diameter between pH 7 and 11, corresponding to more than one order of magnitude difference in volume. Despite the significant difference in size between low and high pH, the size dispersity of the microcapsules in the swollen and nonswollen states remains low.

The trigger-responsive swelling of the shell occurs rapidly upon deprotonation in alkaline conditions. The surface area of the capsule significantly increases within seconds due to the swelling of the shell predominantly in the spherical plane, while the water core volume is initially unchanged; the result is a buckling of the microcapsules immediately after an increase in pH due to the mismatch of surface area to volume of the capsules. The diffusion of water into the capsule core to accommodate the significantly expanded surface area is slow, taking minutes for the cores to be fully filled with water and restore the spherical shape of the microcapsules after a pH-triggered swelling of the shell. Time-resolved microscopy images of microcapsules during the change from their nonswollen state in DI water to their swollen state at pH 9.5 showing the initial buckling of the shell and ultimate recovery are shown in Figure 3b and Video S4 (Supporting Information). Upon a change in pH from basic to acidic conditions the shells turn hydrophobic and deswell, but it takes hours for the capsules to decrease in size. The deswelling of the poly(acid) shells upon

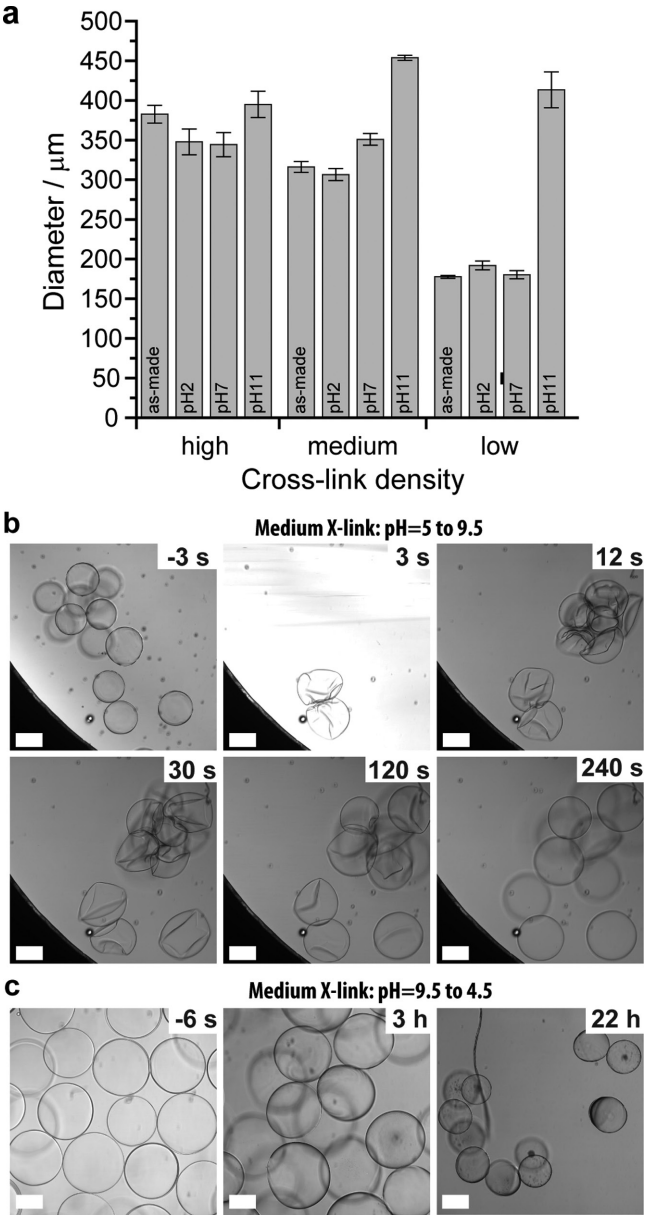

Figure 3. a) Size distribution of microcapsules with high (A-1), medium (B-3), and low (C-2) cross-link density before (as-made) and after hydrolysis at indicated pH values. Values and error bars represent geometric average and standard deviation, respectively, of 3–30 microcapsules. b,c) Time-resolved optical microscopy images of poly(acid) microcapsules with medium cross-link density (B-2) upon pH change from 5 to 9.5 and 9.5 to 4.5. Timestamps in (b) and (c) correspond to the addition of borate buffer (pH = 9.5) and acetate buffer (pH = 4.5), respectively. Scale bars are 200 µm.

protonation of the poly(acid) network drives a decrease in surface area of the microcapsule and, hence, a decrease in volume. However, to decrease the volume of the microcapsules, water has to diffuse from the core through the shell into the continuous medium. Since protonation turns the shells significantly less permeable even to water, the diffusion rate of water is so slow that it takes over 20 h to shrink to their equilibrium size, as shown in Figure 3c. The strain imposed on the shell during

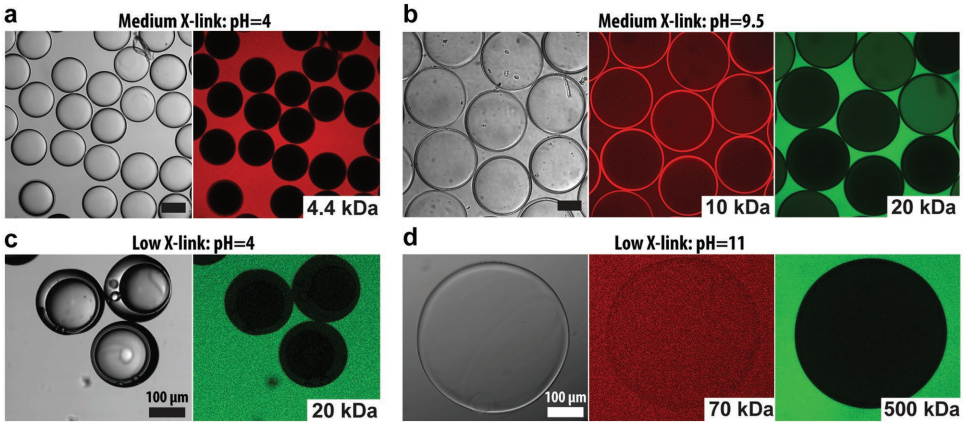

Figure 4. a,b) Bright field (first) and laser confocal fluorescence microscopy images of the same poly(acid) microcapsules (B-3) with medium cross-link density in acidic and alkaline media challenged with fluorescently labeled dextran with indicated molecular weight. Scale bars are 200 µm. c,d) Bright field (first) and laser confocal fluorescence microscopy images of the same poly(acid) microcapsules (C-2) with low cross-link density in acidic and alkaline media challenged with fluorescently labeled dextran with indicated molecular weight.

this slow shrinking process causes some plastic deformation of the capsules after repeated swelling and deswelling cycles, but no ruptured or broken capsules are observed.

The pH-dependent degree of swelling and hydrophilicity allows dynamic control over the permeability of the shell. Deprotonated, swollen microcapsules exhibit higher permeability than in the protonated, nonswollen state. The MWCO of substances below which the poly(acid) shells are permeable in the swollen and nonswollen states is precisely tunable through the cross-link density; the MWCO increases with decreasing cross-link density due to a larger mesh size in the polymeric network. For example, microcapsules with medium cross-link density are impermeable to fluorescently labeled dextran with a molecular weight of 4.4 kg mol^{-1} at pH 4, but the same microcapsules are permeable to molecular weights up to 10 kg mol^{-1} at pH 9.5, as shown in the confocal fluorescence microscopy images in **Figure 4**a,b. In comparison, microcapsules with low cross-link density are impermeable to dextran with a molecular weight of 20 kg mol^{-1} in their nonswollen state in acidic media, but permeable to molecular weights up to 70 kg mol^{-1} when swollen at high pH, yet remain impermeable to larger molecular weights, confirming that the capsules are free of larger defects or ruptures, as shown in Figure 4c,d. Microcapsules with high cross-link density are impermeable to macromolecules such as fluorescently labeled dextran with a molecular weight down to 4.4 kg mol^{-1} at any pH, but demonstrate pH and solute size dependent diffusion rates of small sugar molecules. To assess their permeability, the highly cross-linked microcapsules are exposed to sugar solutions of high concentration at various pH. The resultant osmotic pressure causes an immediate water diffusion from the capsule core to the surrounding sugar solution; the result is a buckling of the microcapsules due to the decreased core volume but unchanged surface area. The lower the permeability of the shell membrane to the sugar, the longer it takes to equilibrate the osmolarity inside and outside of the capsule, and hence the time until its spherical shape is restored. Osmotic shock experiments in various pH conditions demonstrate the permeability of the highly cross-linked poly(acid) microcapsules to sucrose and cyclodextrin with molecular weights of up to 1297 g mol^{-1} at neutral and high pH, but significantly lower permeability in acidic conditions with recovery times of weeks, as summarized in Figure S5 (Supporting Information).

2.4. Reversible Permeability Switching of the Dynamic Microcapsules

The pH-dependent swelling and associated permeability change is reversible, which enables the use of these capsules for more advanced functions than the common single-use, unidirectional delivery applications. Release profiles that adapt to a changing environment can be obtained with microcapsules that sense their surrounding and modify their permeability in response to changes. Additionally, manipulation of the microcapsule environment allows active on-off switching and release control, as schematically shown in **Figure 5**. The dynamic change of the permeability triggered by a change in pH is utilized to temporarily interrupt the release of cargo from the capsules, demonstrating active and repeated on-off release manipulation of the microcapsules by an external trigger. Capsules with medium cross-link density are loaded with fluorescein-labeled dextran with a molecular weight of 10 kg mol^{-1} and successively exposed to basic and acidic conditions, while the absorbance of the supernatant is measured to assess the release of the encapsulated dextran over time. During exposure of the microcapsules to alkaline conditions, the absorbance of fluorescein in the supernatant increases continuously over 10 min, demonstrating release of the fluorescent cargo. Upon acidification of the aqueous medium, the absorbance of the supernatant barely changes for over 45 min, while it significantly increases again over the next 10 min when the pH is switched back to 9, as shown in Figure 5. This process can be repeated for another cycle, interrupting and continuing the release of the dextran again with acid and base, respectively. The peak absorbance of the supernatant over time under cycled pH conditions is shown in Figure 5, and the absorption spectra of the supernatant during release in alkaline conditions

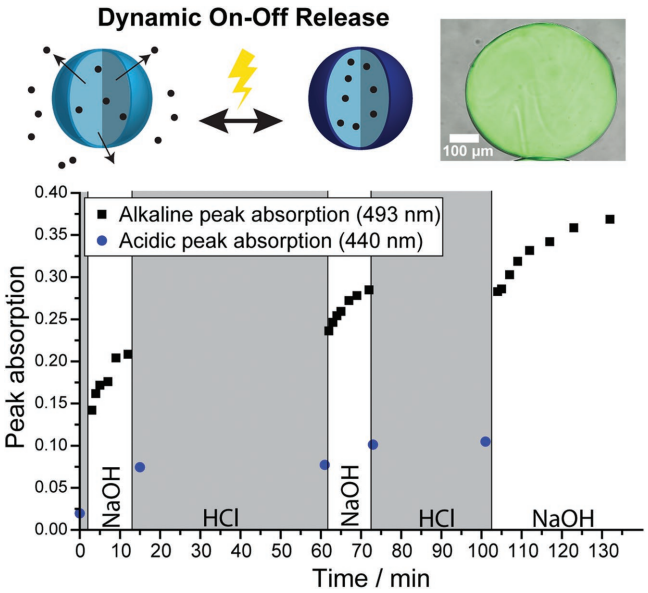

Figure 5. Illustration of dynamic on-off release (top) and time-resolved peak absorption (bottom) of the supernatant over microcapsules (B-2) loaded with FITC-labeled dextran (10 kDa) during pH-triggered on-off release, demonstrating the repeated change of permeability of the microcapsules upon switching between acidic and alkaline conditions. The inset (top right) shows an overlay of the bright field and fluorescence confocal microscopy image of a loaded microcapsule before dynamic release.

are plotted in Figure S6c (Supporting Information). Since the fluorescein-labeled dextran exhibits pH-dependent absorption spectra, comparison can only be made between absorption values for the same pH conditions. No increase in absorption is observed in acidic conditions, demonstrating no release during an acidic cycle, while the absorption increases fast and significantly during all basic cycles, demonstrating the repeatedly activated release. The repeated and rapid on-off switching of the release demonstrates the dynamic responsiveness to control the shell permeability without destruction of its structural integrity.

Since the change of the permeability is nondestructive, cargo can be loaded into the capsules while permeable at high pH, trapped in the capsules at low pH, and successively released again at high pH, as illustrated in **Figure 6**a. Capture, trapping, and release of cargo molecules in the dynamically responsive microcapsules are visualized using fluorescently labeled dextran with molecular weight of 10 kg mol^{-1}. The probe diffuses into the capsules in alkaline conditions and stays trapped inside when the capsules are transferred to acidic conditions. After increase of the pH, the dextran is fully released from the capsules over a period of 20 min, as summarized in Figure 6a. Time-resolved intensity profiles across a releasing capsule demonstrating the continued and full release of the fluorescent cargo molecule over 20 min are shown in Figure S6a (Supporting Information). The time for capture and release depends on the diffusion rate through the shell membrane; small molecules diffuse faster. The same poly(acid) shells are impermeable to 4.4 kg mol^{-1} dextran for days at low pH, but diffusion into the capsules is completed within 2 min when the pH is changed to 9.5, as shown in Figure 6b. The shells become impermeable again within seconds after the pH is switched to 4, exhibiting no release of the trapped dextran immediately following acidification of the surrounding liquid. Time-resolved fluorescent confocal microscopy images of the blocking, capture, and trapping of 4.4 kg mol^{-1} dextran are summarized in Figure 6b and shown in Videos S5 and S6 (Supporting Information). The difference of diffusion rate of the two molecular probes is shown in the diffusion profiles plotted in Figure 6b. While the 10 kDa dextran requires 1200 s to reach 80% equilibrium of the fluorescence inside and outside the capsule, it only takes 150 s for the 4.4 kDa dextran.

The fast response time and the significant change in permeability of the capsules is due to a substantial difference in hydrophilicity between the protonated and the deprotonated ionic state of the polymer networks. The permeability of the protonated state is so low that it takes hours for the microcapsules to reach their nonswollen size due to the very slow diffusion of water from the core through the hydrophobic shell. We associate the robust mechanical properties of the capsules, and their ability to withstand the significant stresses that evolve during this deswelling, to the very homogeneous polymeric networks obtained from thiol–ene chemistry.[32]

In addition to pH, the poly(acid) microcapsules are responsive to changes in their ionic environment. Multivalent cations such as calcium(II) physically cross-link deprotonated poly(acids). In alkaline conditions, the addition of calcium chloride leads to deswelling of the shells and associated permeability change, similar to the demonstrated dynamic response to acid. Fluorescently labeled 4.4 kg mol^{-1} dextran is captured in microcapsules with medium cross-link density at a pH of 9.5, and trapped for hours at the same pH upon addition of 0.1 molar calcium chloride that causes a decrease in capsule size, as shown in Figure 6c. The calcium is removed from the poly(acid) shells through the addition of a competing chelating agent such as ethylenediaminetetraacetic acid (EDTA), causing a reswelling of the microcapsules with associated MWCO increase. After addition of excess EDTA, the trapped dextran is released, and the capsule size increases again. The calcium response enables the same capture-trap-release capability of the poly(acid) microcapsules as for changes between acidic and alkaline pH conditions, but without pH-change, as summarized in the fluorescence confocal microscopy images in Figure 6c.

The mechanical robustness of the microcapsules is also apparent in their stability upon drying. Poly(anhydride) microcapsules that are dried in vacuum at room temperature aggregate and adhere to each other, but retain nonvolatile cargo such as the fluorescent probe sulforhodamine B. Upon redispersing the poly(anhydride) microcapsules in aqueous medium, the cargo stays trapped within the capsules until they are hydrolyzed and allow diffusion of the probe through the shell, as shown in Figure S7a (Supporting Information). The capsules can further be detached from each other with light ultrasonication and the hydrolyzed microcapsules retain their pH-responsiveness as demonstrated by the trapping of 4.4 kDa dextran in Figure S7b (Supporting Information) upon pH change from basic to acidic medium.

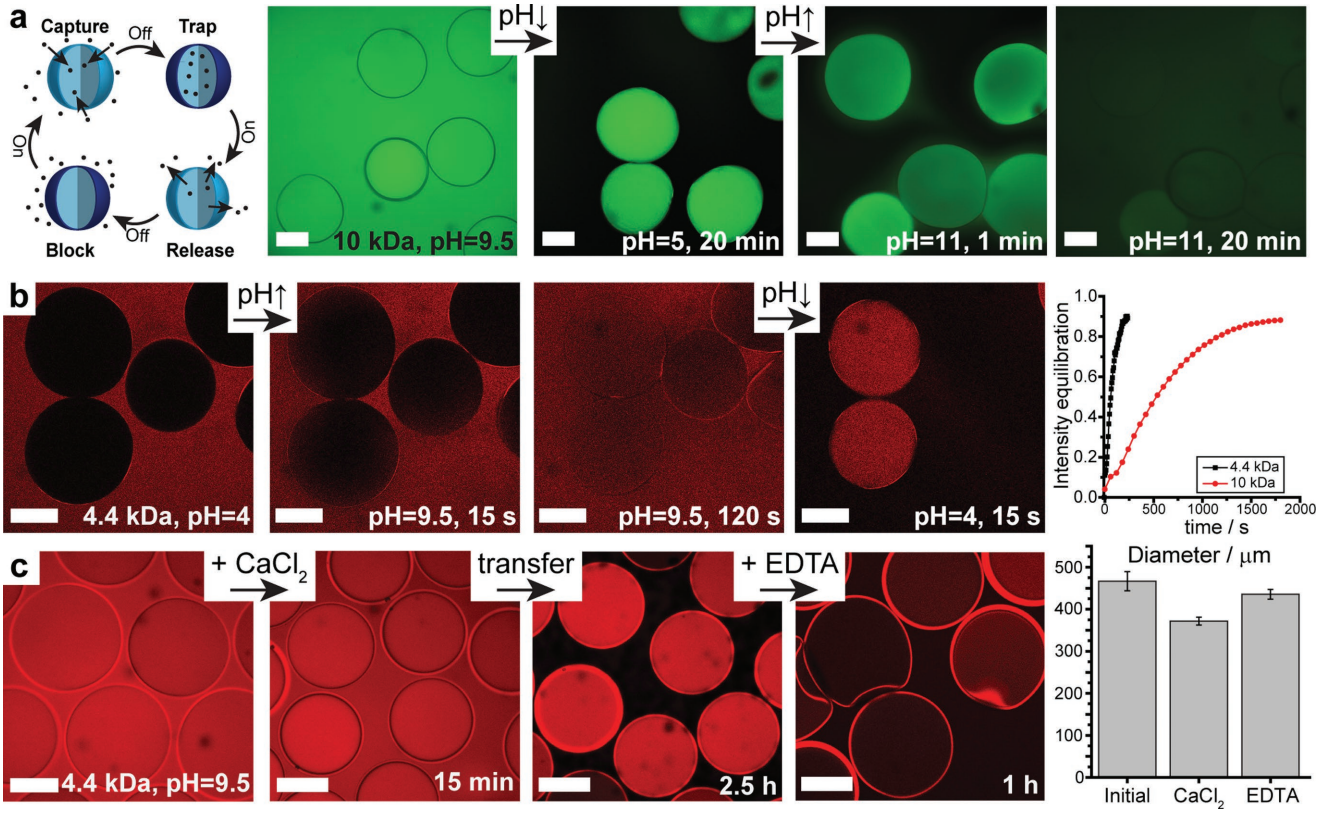

Figure 6. a,b) Laser confocal fluorescence microscopy images of microcapsules (B-2) during a pH-triggered capture-trap-release and block-capture-trap cycle of fluorescently labeled dextran (a: 10 kDa; b: 4.4 kDa) at indicated conditions and times. Graph in (b) shows the time-resolved ratio of average intensities between the high and low concentration of the fluorescent probes from one of the capsules during release in (a) and capture in (b) (areas indicated in Figure S6, Supporting Information). c) Laser confocal fluorescence microscopy images of microcapsules (B-3) during a calcium-triggered capture-trap-release cycle of fluorescently labeled dextran (4.4 kDa) at indicated conditions and times. All scale bars are 200 µm.

3. Conclusion

Herein, we demonstrate a new class of microcapsules with dynamic permeability that switches on and off within seconds, enabling the microcapsules to transiently release cargo with actively induced interruptions by controlling the environmental pH or ionic species. The release rate is controllable through molecular composition of the microcapsules, enabling their precise task-specific tunability. Due to their small size, microcapsules can be used as injectable drug reservoirs that release their aqueous cargo only under predetermined conditions with precisely tunable rates. Furthermore, biologics that produce therapeutics on-site such as enzymes, proteins, or even cells could be directly incorporated and hosted as unperturbed cargo in the microcapsule since the core constitutes liquid water physically separated from the encapsulation material. The cargo is protected from certain immune responses by the shell membrane, while the supply of substrate molecules and release of products is controlled by the environmental conditions, enabling on-demand and on-site production of therapeutics. Furthermore, the dynamic microcapsules can repeatedly capture molecular species from their surrounding aqueous medium with size selectivity and trap them without leakage, enabling new methods for passive and active separation and purification with facile removal of molecular impurities by microfiltration or gravitational settling.

4. Experimental Section

Chemicals: PenAn, TEGDVE, PETMP, poly(vinyl alcohol) (M_w 13 000–23 000, 98% hydrolyzed, PVA), 2-hydroxy-2-methylpropiophenone (Darocure 1173), acetic acid (glacial), sodium hydroxide (pellets, NaOH), hydrochloric acid (2 N, HCl), sodium phosphate monobasic (dihydrate), sodium borate, sodium phosphate dibasic (dodecahydrate), PBS (1×), calcium chloride, EDTA, and octadecyltrimethoxysilane (technical grade, 90%, ODTS) were purchased from Sigma-Aldrich and used as received. The fluorescent probes sulforhodamine B, rhodamine isothiocyanate-dextran (RITC-dextran), and fluorescein isothiocyanate-dextran (FITC-dextran) of various molecular weights were purchased from Sigma-Aldrich and used as received as 1 mg mL^{-1} solutions in DI water. The hydrophilic silane 2-(methoxy-(polyethyleneoxy)propyl) trimethoxysilane was purchased from Gelest and used as received. Hydrolysis and size distribution measurements at pH 2, pH 4, and pH 11 were done with BDH pH Reference Standard Buffers or with PBS buffer for pH 7. Osmotic shock and capture-trap-release experiments were done with 0.02 M solutions at appropriate ratios of acetic acid and sodium hydroxide for pH 4, and sodium phosphate mono- and dibasic for pH 7, and sodium borate for pH 9.5.

Preparation of Monomer Mixtures: Hydrophobic thiol–ene monomer mixtures with a stochiometric ratio of double bonds (ene) to thiols were used as the shell phase in microfluidic double emulsion drop templating. Three monomer compositions were prepared with PETMP as the multifunctional thiol and PenAn and TEGDVE as the difunctional enes with 14.3, 33.3, and 60 mol% PenAn in the ene mixture, corresponding to 25, 50, and 90 mol% of acid groups in the fully hydrolyzed shells as compared to TEGDVE, as summarized in Table 1. The radical photoinitiator 2-hydroxy-2-methylpropiophenone (Darocure

1173) was added at 1 mole% to the monomer mixtures. The monomers were prepared and mixed by shaking immediately before use.

Fabrication of Microcapsules in Microfluidic Dropmakers: Microcapsules were produced from double emulsion templates with an aqueous core consisting of 2–5 wt% PVA, optionally containing sulforhodamine B at 0.1 mg mL^{-1}. The continuous phase consists of 5 wt% PVA. Water-in-oil-in-water double emulsions were fabricated using a glass capillary microfluidic device, as illustrated in Scheme S1 (Supporting Information). The device consists of two tapered cylindrical capillaries aligned inside a square capillary with dimensions slightly larger than that of the outer diameter of the cylindrical capillaries. The injection capillary was rendered hydrophobic by treating it with ODTS. To prevent the wetting of the shell of the double emulsion drops on the outlet channel walls, the collection capillary was rendered hydrophilic by treating with 2-(methoxy-(polyethyleneoxy)propyl)trimethoxysilane. For thin shell capsules, an additional flame-pulled cylindrical capillary was inserted into the hydrophobic injection capillary.

To form thick-shell double emulsion drops, the inner aqueous phase was injected through the hydrophobically treated injection capillary, while the middle shell phase was injected from the same direction through the interstitial space between the square capillary and the injection capillary. The outer aqueous phase was injected from the opposite direction, also through the interstitial space between the square capillary and collection capillary. Thin-shell double emulsion drops were obtained by injecting the inner aqueous phase through the flame-pulled innermost capillary, the monomer middle phase through the injection capillary, and the aqueous outer phase through the interstitial space between the square and the collection capillary, as illustrated in Scheme S1 (Supporting Information). Drop formation in the glass capillary device was monitored with a fast camera (Phantom V9.0) equipped onto a Leica inverted optical microscope. Double emulsion drops were formed in the dripping regime at various flow rates, as summarized in Table 1. Following drop breakup, the double emulsion drops flowed through the cylindrical collection capillary and were immediately irradiated with UV light (OmiCure S1500, 320–500 nm filter) to photopolymerize the shells. The microcapsules were collected in a vial containing 5 wt% PVA in water.

Hydrolysis of Microcapsules: The hydrolysis of the poly(PenAn-TEGDVE-PETMP) microcapsules was performed under various pH conditions. To monitor the hydrolysis, small aliquots of microcapsules (≈20 µL) were placed into buffer solutions (200 µL) of pH 2, 7, 11, or in DI water (pH ≈ 5). For microcapsules that did not contain sulforhodamine B dye in their core, it was added to the buffers in the wells. Hydrolyzed poly(acid) shells allow the diffusion of sulforhodamine B through the shell membrane, while the unhydrolyzed poly(anhydride) shells are impermeable to this probe molecule. Completion of the hydrolysis of the poly(anhydride) network is confirmed by observing the diffusion of sulforhodamine B dye through the shell membrane using a laser confocal fluorescent microscope (Leica Microsystems) over a period of several days.

Characterization of Microcapsules: Microcapsules for Fourier-transform infrared (FT-IR) spectroscopy and SEM analysis were prepared by washing aliquots of microcapsules four times with DI water, and drying under vacuum. FT-IR measurements were performed using a Bruker FTIR microscope (Lumos) in attenuated total reflectance (ATR) mode. Some dried microcapsules for SEM were cross-sectioned with a razor blade after depositing the microcapsules onto double-sided adhesive conductive carbon tape. Prior to imaging, the SEM samples were sputter-coated with a thin layer (5 nm) of platinum/palladium (Pt:Pd 80:20) using a sputter coater (EMS 300T D Dual Head Sputter Coater). The microcapsules were imaged using a field emission scanning electron microscope (FESEM, Zeiss UltraPlus) equipped with an in-lens detector.

Permeability Measurements: Microcapsule permeability and MWCO of the poly(acid) shells with medium and low cross-link density (entries B and C in Table 1) under various pH conditions were characterized using molecular permeation into the capsule interior of fluorescent dye-conjugated dextran with various molecular weights at concentrations of 1 mg mL^{-1}. To a well containing the microcapsules in the respective buffer solution (100 µL) of desired pH, the dye-dextran solution was added (20 µL) and incubated for at least 1 h. For microcapsules with high cross-link density (entry A in Table 1), pH-dependent permeability changes were gauged using osmotic shock response with sugar molecules. Solutions of sucrose and γ-cyclodextrin (γ-CD) were prepared at concentrations of 200 g L^{-1} and added to aliquots of the microcapsules in buffer solutions of pH 4, pH 7, and pH 11. During the permeability experiments, the capsules were characterized and monitored using a laser confocal fluorescent microscope (Leica Microsystems).

Dynamic Switching of Microcapsules: Actively adjustable release was demonstrated with microcapsules of medium cross-link density (entry B-2 in Table 1). To load the capsules with the fluorescent cargo probe, microcapsules were placed into borate buffer solution containing 10 kDa FITC-dextran with a pH of 9.5 for 3 h. The supernatant was acidified with 1 M HCl (pH = 4) and washed five times with DI water. The capsules were transferred to an acidic mixture of 0.02 M glycine and 0.025 M HCl, in which no dye release was observed for 18 h. The capsule dispersion was transferred into a quartz glass cuvette and placed in an Agilent Cary 50 UV–vis spectrophotometer. To enable and disable release from the capsules, 1 M NaOH and HCl (20–30 µL) were added, respectively, while measuring the absorption spectrum of the supernatant above the settled capsules frequently.

Capture, trap, and release experiments were performed with microcapsules of medium cross-link density (entries B in Table 1) in 200 µL wells and monitored with laser confocal fluorescence microscopy (Leica Microsystems). Aliquots of the microcapsules were added to buffer-filled wells together with fluorescently labeled dextran of respective molecular weights. Capture, trapping, and release were achieved by either replacing the supernatant with a buffer solution of the desired pH, or desired salt solution (0.1 M calcium chloride or sodium EDTA in borate buffer with a pH of 9.5).

Supporting Information

Supporting Information is available from the Wiley Online Library or from the author.

Acknowledgements

This work was supported by the National Science Foundation (DMR-1708729). This work was performed in part at the Harvard MRSEC (Grant No. DMR-1420570) and the Center for Nanoscale Systems (CNS), a member of the National Nanotechnology Coordinated Infrastructure Network (NNCI), which was supported by the National Science Foundation under NSF Award No. 1541959. CNS is part of Harvard University.

Conflict of Interest

The authors declare no conflict of interest.

Keywords

actuation, microcapsules, microfluidics, stimuli-responsive capsules, thiol–ene

Received: May 16, 2018
Revised: June 30, 2018
Published online:

[1] R. P. John, R. D. Tyagi, S. K. Brar, R. Y. Surampalli, D. Prévost, *Crit. Rev. Biotechnol.* **2011**, *31*, 211.
[2] I. M. Martins, M. F. Barreiro, M. Coelho, A. E. Rodrigues, *Chem. Eng. J.* **2014**, *245*, 191.

[3] S. Mitragotri, P. A. Burke, R. Langer, *Nat. Rev. Drug Discovery* **2014**, *13*, 655.
[4] A. Gharsallaoui, G. Roudaut, O. Chambin, A. Voilley, R. Saurel, *Food Res. Int.* **2007**, *40*, 1107.
[5] T. M. S. Chang, *Science* **1964**, *146*, 524.
[6] S. S. Datta, A. Abbaspourrad, E. Amstad, J. Fan, S.-H. Kim, M. Romanowsky, H. C. Shum, B. Sun, A. S. Utada, M. Windbergs, S. Zhou, D. A. Weitz, *Adv. Mater.* **2014**, *26*, 2205.
[7] S. Benita, *Microencapsulation: Methods and Industrial Applications*, CRC Press, Boca Raron, FL **2006**.
[8] X. Wang, J. Feng, Y. Bai, Q. Zhang, Y. Yin, *Chem. Rev.* **2016**, *116*, 10983.
[9] A. Abbaspourrad, N. J. Carroll, S. H. Kim, D. A. Weitz, *J. Am. Chem. Soc.* **2013**, *135*, 7744.
[10] A. Abbaspourrad, S. S. Datta, D. A. Weitz, *Langmuir* **2013**, *29*, 12697.
[11] J. Kost, R. Langer, *Adv. Drug Delivery Rev.* **2012**, *64*, 327.
[12] K. Ishihara, M. Kobayashi, N. Ishimaru, I. Shinohara, *Polym. J.* **1984**, *16*, 625.
[13] M. J. Zhang, W. Wang, R. Xie, X. J. Ju, L. Liu, Y. Y. Gu, L. Y. Chu, *Soft Matter* **2013**, *9*, 4150.
[14] E. Mathiowitz, R. Langer, *J. Controlled Release* **1987**, *5*, 13.
[15] H. B. Park, J. Kamcev, L. M. Robeson, M. Elimelech, B. D. Freeman, *Science* **2017**, *356*, eaab0530.
[16] A. Abbaspourrad, N. J. Carroll, S. H. Kim, D. A. Weitz, *Adv. Mater.* **2013**, *25*, 3215.
[17] S. Tang, L. Tang, X. Lu, H. Liu, J. S. Moore, *J. Am. Chem. Soc.* **2018**, *140*, 94.
[18] G. Li, G. Liu, E. Kang, K. Neoh, X. Yang, *Langmuir* **2008**, *24*, 9050.
[19] W. Tong, C. Gao, H. Möhwald, *Macromolecules* **2006**, *39*, 335.
[20] C. Djugnat, G. B. Sukhorukov, *Langmuir* **2004**, *20*, 7265.
[21] J. Wei, X.-J. Ju, R. Xie, C.-L. Mou, X. Lin, L.-Y. Chu, *J. Colloid Interface Sci.* **2011**, *357*, 101.
[22] J. S. Sander, M. Steinacher, E. Loiseau, A. F. Demirörs, M. Zanini, L. Isa, A. R. Studart, *Langmuir* **2015**, *31*, 6965.
[23] V. Kozlovskaya, E. Kharlampieva, M. L. Mansfield, S. A. Sukhishvili, *Chem. Mater.* **2006**, *18*, 328.
[24] M. A. C. Stuart, W. T. S. Huck, J. Genzer, M. Müller, C. Ober, M. Stamm, G. B. Sukhorukov, I. Szleifer, V. V. Tsukruk, M. Urban, F. Winnik, S. Zauscher, I. Luzinov, S. Minko, *Nat. Mater.* **2010**, *9*, 101.
[25] T. Y. Lee, T. M. Choi, T. S. Shim, R. A. M. Frijns, S.-H. Kim, *Lab Chip* **2016**, *16*, 3415.
[26] R. K. Shah, H. C. Shum, A. C. Rowat, D. Lee, J. J. Agresti, A. S. Utada, L. Y. Chu, J. W. Kim, A. Fernandez-Nieves, C. J. Martinez, D. A. Weitz, *Mater. Today* **2008**, *11*, 18.
[27] K. L. Poetz, H. S. Mohammed, B. L. Snyder, G. Liddil, D. S. K. Samways, D. A. Shipp, *Biomacromolecules* **2014**, *15*, 2573.
[28] B. S. Kim, J. S. Hrkach, R. Langer, *J. Polym. Sci., Part A: Polym. Chem.* **2000**, *38*, 1277.
[29] A. S. Utada, E. Lorenceau, D. R. Link, P. D. Kaplan, H. A. Stone, D. A. Weitz, *Science* **2005**, *308*, 537.
[30] L. R. Arriaga, E. Amstad, D. A. Weitz, *Lab Chip* **2015**, *15*, 3335.
[31] W. J. Duncanson, T. Lin, A. R. Abate, S. Seiffert, R. K. Shah, D. A. Weitz, *Lab Chip* **2012**, *12*, 2135.
[32] C. E. Hoyle, T. Y. Lee, T. Roper, *J. Polym. Sci., Part A: Polym. Chem.* **2004**, *42*, 5301.